

# 2

---

## Fundamentals of Chemical Vapor Deposition

---

### 1.0 INTRODUCTION

Chemical vapor deposition is a synthesis process in which the chemical constituents react in the vapor phase near or on a heated substrate to form a solid deposit. The CVD technology combines several scientific and engineering disciplines including thermodynamics, plasma physics, kinetics, fluid dynamics, and of course chemistry. In this chapter, the fundamental aspects of these disciplines and their relationship will be examined as they relate to CVD.

The number of chemical reactions used in CVD is considerable and include thermal decomposition (pyrolysis), reduction, hydrolysis, disproportionation, oxidation, carburization, and nitridation. They can be used either singly or in combination (see Ch. 3 and 4). These reactions can be activated by several methods which are reviewed in Ch. 5. The most important are as follows:

- Thermal activation which typically takes place at high temperatures, i.e.,  $>900^{\circ}\text{C}$ , although the temperature can also be lowered considerably if metallo-organic precursors are used (MOCVD).

- Plasma activation which typically takes place at much lower temperatures, i.e., 300–500°C.
- Photon activation, usually with shortwave ultraviolet radiation, which can occur by the direct activation of a reactant or by the activation of an intermediate .

Until recently, most CVD operations were relatively simple and could be readily optimized experimentally by changing the reaction chemistry, the activation method, or the deposition variables until a satisfactory deposit was achieved. It is still possible to do just that and in some cases it is the most efficient way to proceed. However, many of the CVD processes are becoming increasingly complicated with much more exacting requirements, which would make the empirical approach too cumbersome.

### **1.1 Theoretical Analysis**

A theoretical analysis is, in most cases, an essential step which, if properly carried out, should predict any of the following:

- Chemistry of the reaction (intermediate steps, by-products).
- Reaction mechanism.
- Composition of the deposit (i.e., stoichiometry).
- Structure of the deposit (i.e., the geometric arrangement of its atoms).

This analysis may then provide a guideline for an experimental program and considerably reduce its scope and save a great deal of time and effort.

Such an analysis requires a clear understanding of the CVD process and a review of several fundamental considerations in the disciplines of thermodynamics, kinetics, and chemistry is in order. It is not the intent here to dwell in detail on these considerations but rather provide an overview which should be generally adequate. More detailed investigations of the theoretical aspects of CVD are given in Refs. 1–3.

## 2.0 THERMODYNAMICS OF CVD

A CVD reaction is governed by *thermodynamics*, that is the driving force which indicates the direction the reaction is going to proceed (if at all), and by *kinetics*, which defines the transport process and determines the rate-control mechanism, in other words, how fast it is going.

Chemical thermodynamics is concerned with the interrelation of various forms of energy and the transfer of energy from one chemical system to another in accordance with the first and second laws of thermodynamics. In the case of CVD, this transfer occurs when the gaseous compounds, introduced in the deposition chamber, react to form the solid deposit and by-products gases.

### 2.1 $\Delta G$ Calculations and Reaction Feasibility

The first step of a theoretical analysis is to ensure that the desired CVD reaction will take place. This will happen if the thermodynamics is favorable, that is if the transfer of energy—the free-energy change of the reaction known as  $\Delta G_r$ —is negative. To calculate  $\Delta G_r$ , it is necessary to know the thermodynamic properties of each component, specifically their free energies of formation (also known as Gibbs free energy),  $\Delta G_f$ . The relationship is expressed by the following equation:

$$\text{Eq. (1)} \quad \Delta G_r^\circ = \sum \Delta G_f^\circ \text{ products} - \sum \Delta G_f^\circ \text{ reactants}$$

The free energy of formation is not a fixed value but varies as a function of several parameters which include the type of reactants, the molar ratio of these reactants, the process temperature, and the process pressure. This relationship is represented by the following equation:

Eq. (2)  $\Delta G_r = \Delta G_f^o + RT \ln Q$

where:

$$\Delta G_r^o = \sum z_i^i \Delta G_{f,i}^o$$

$z_i$  = stoichiometric coefficient of species “i” in the CVD reaction (negative for reactants, positive for products)

$\Delta G_{f,i}^o$  = standard free energy of formation of species “i” at temperature  $T$  and 1 atm.

$R$  = gas constant

$T$  = absolute temperature

$$Q = \prod_i a_i^{z_i}$$

$a_i$  = activity of species “i” which is = 1 for pure solids and =  $p_i = x_i P_T$  for gases

$p_i$  = partial pressure of species “i”

$x_i$  = mole fraction of species “i”

$P_T$  = total pressure

By definition, the free energy change for a reaction at equilibrium is zero, hence:

Eq. (3)  $\Delta G = - RT \ln K$   
( $K$  is the equilibrium constant)

It is the equilibrium conditions of composition and activities (partial pressure for gases) that are calculated to assess the yield of a desired reaction.

A demonstration of the feasibility of a reaction is illustrated in the following example regarding the formation of titanium diboride using either diborane or boron trichloride as a boron source, as shown in the following reactions:



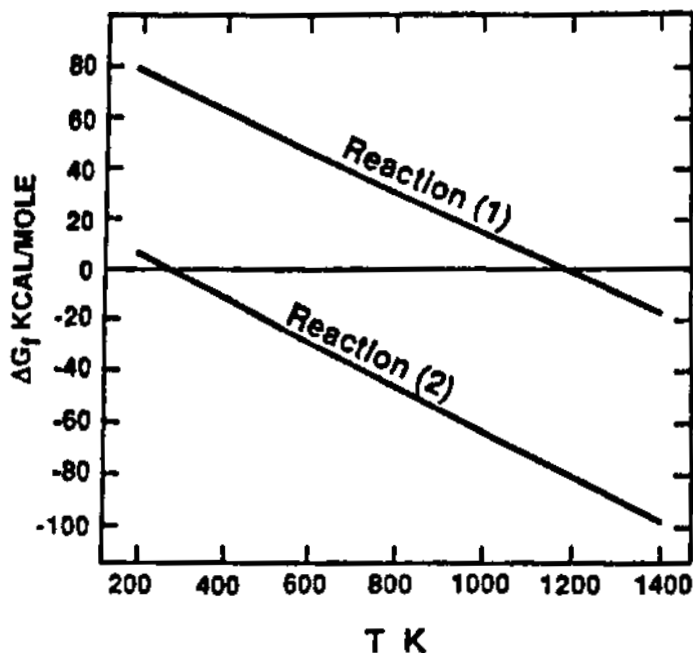


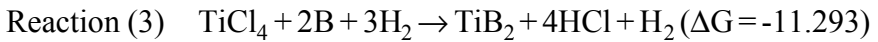
**Figure 2.1.** Changes in free energy of formation for  $\text{TiB}_2$  deposition in the following reactions: (1)  $\text{TiCl}_4 + 2\text{BCl}_3 \rightarrow \text{TiB}_2 + 10\text{HCl}$ ; (2)  $\text{TiCl}_4 + \text{B}_2\text{H}_6 \rightarrow \text{TiB}_2 + \text{H}_2$ .

The changes in free energy of formation of Reaction (1) are shown in Fig. 2.1 as a function of temperature.<sup>[4]</sup> The values of  $\Delta G_r$  were calculated using Eq. (1) above for each temperature. The Gibbs free-energy values of the reactants and products were obtained from the JANAF Tables.<sup>[5]</sup> Other sources of thermodynamic data are listed in Ref. 6. These sources are generally accurate and satisfactory for the thermodynamic calculations of most CVD reactions; they are often revised and expanded.

$\text{TiB}_2$  can also be obtained using diborane as a boron source as follows:



The changes in the free energy of formation on this reaction are shown in Fig. 2.1. It should be noted that the negative free energy change is a valid criterion for the feasibility of a reaction only if the reaction, as written, contains the major species that exist at equilibrium. In the case of Reaction (2), it is possible that  $B_2H_6$  has already decomposed to boron and hydrogen and the equilibrium of the reaction might be closer to:



As can be seen in Fig. 2.1, if the temperature is raised sufficiently,  $\Delta G_r$  becomes negative and the diborane reaction proceeds at a much lower temperature than the boron trichloride reaction.

## **2.2 Thermodynamic Equilibrium and Computer Programs**

Reactions (1) and (2) above are actually greatly simplified. In reality, it is likely that subchlorides such as  $TiCl_3$  and  $TiCl_2$  will be formed in Reaction (1) and higher boranes in Reaction (2). Such factors are not revealed by the simple free-energy change calculations.

In many cases, a more complete understanding of CVD reactions and a better prediction of the results are needed and a more thorough thermodynamic and kinetic investigation is necessary. This is accomplished by the calculation of the thermodynamic equilibrium of a CVD system, which will provide useful information on the characteristics and behavior of the reaction, including the optimum range of deposition conditions.

The calculation is based on the rule of thermodynamics, which states that a system will be in equilibrium when the Gibbs free energy is at a minimum.<sup>[7]</sup> The objective then is the minimization of the total free energy of the system and the calculation of equilibria at constant temperature and volume or at constant pressure.<sup>[8]</sup> It is a complicated and lengthy calculation but, fortunately, several computer programs are now available that considerably simplify the task.<sup>[9]</sup>

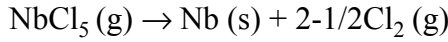
Such programs include SOLGASMIX, which was developed by Erikson and Besmann<sup>[10][11]</sup> and EKVICALC and EKVIBASE, developed by Nolang.<sup>[12]</sup> These programs are now used widely in equilibrium calculations in CVD systems. To operate them, it is first necessary to identify all the possible chemical species, whether gaseous or condensed phases, that might be found in a given reaction. The relevant thermodynamic properties of these phases are then entered in the program as input data. If properly performed, these calculations will provide the following information:

- The composition and amount of deposited material that is theoretically possible under any given set of deposition conditions, that is at a given temperature, a given pressure and given input concentration of reactants.
- The existence of gaseous species and their equilibrium partial pressures.
- The possibility of multiple reactions and the number and composition of possible solid phases, with the inclusion of the substrate as a possible reactant.
- The likelihood of a reaction between the substrate and the gaseous or solid species.

All of this is valuable information, which can be of great help. Yet, it must be treated with caution since, in spite of all the progress in thermodynamic analysis, the complexity of many CVD reactions, is such that predictions based on thermodynamic calculations, are still subject to uncertainty. As stated above, these calculations are based on chemical equilibrium which is rarely attained in CVD reactions.

It follows that, in order to provide a reliable and balanced investigation, it is preferable to combine the theoretical calculations with an experimental program and, hopefully, they will correlate. Fortunately, laboratory CVD experiments are relatively easy to design and carry out; they do not require expensive equipment and results can usually be obtained quickly and reliably.

A classic example, combining theoretical study and laboratory experiments, is the deposition of niobium, originally described by Blocher.<sup>[13]</sup> The following reaction was used:



In Fig. 2.2, the critical deposition temperature of  $\text{NbCl}_5$ , as a function of its initial pressure, is shown from experimental data from Blocher and the author. There are two temperature-pressure regions, which are separated by a straight line. The metal is deposited only in the region below the line. Above, there is no deposition. The line is a least-square fit of the data. Its position was confirmed using the SOLGASMIX computer program.

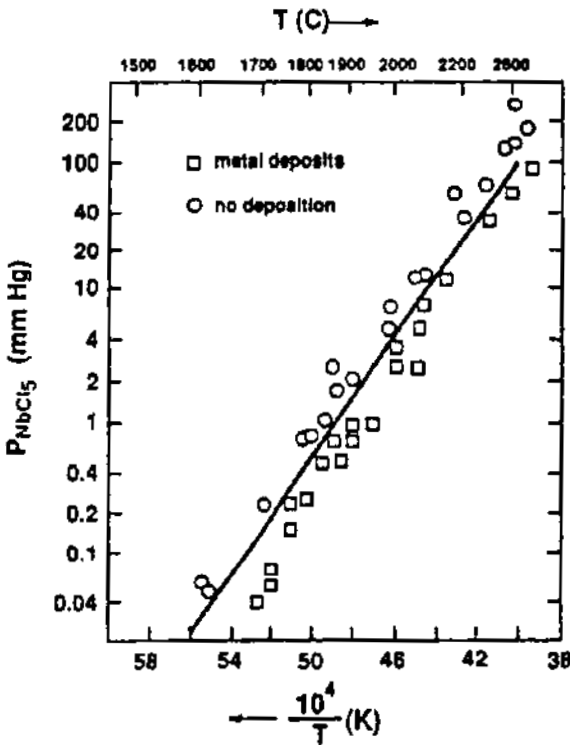


**Figure 2.2.** Critical deposition temperature of niobium as a function of  $\text{NbCl}_5$  initial pressure.

This example shows the great degree of flexibility that can be obtained in CVD if a proper understanding of the thermodynamics and kinetics is gained. In this particular case, it was possible to deposit a uniform layer of NbC on a graphite rod simply by limiting the reaction to the deposition of the metal. Since the carbide could only be formed using the substrate as a carbon source, the rate was controlled by the diffusion rate of the carbon through the coating and deposition uniformity was achieved over the length of the graphite rod.

### **3.0 KINETICS AND MASS-TRANSPORT MECHANISMS**

#### **3.1 Deposition Sequence**

As shown above, a thermodynamic analysis indicates what to expect from the reactants as they reach the deposition surface at a given temperature. The question now is, how do these reactants reach that deposition surface? In other words, what is the mass-transport mechanism? The answer to this question is important since the phenomena involved determines the reaction rate and the design and optimization of the CVD reactor.

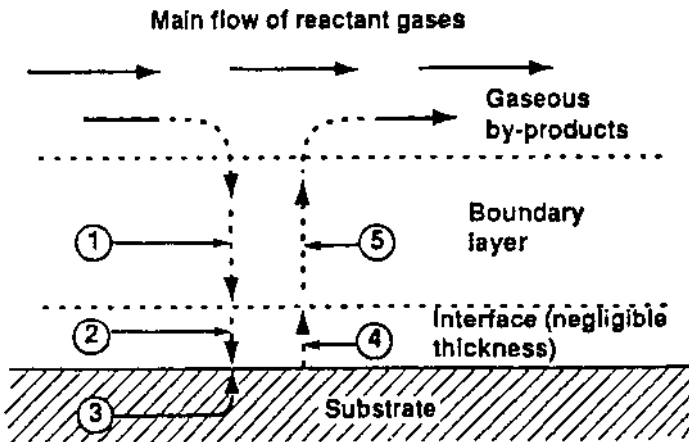
It should be first realized that any CVD process is subject to complicated fluid dynamics. The fluid, in this case a combination of gases, is forced through pipes, valves, and various chambers and, at the same time, is the object of large variations in temperature and to a lesser degree of pressure before it comes in contact with the substrate where the deposition reaction takes place. The reaction is heterogeneous which means that it involves a change of state, in this case from gaseous to solid.

In some cases, the reaction may take place before the substrate is reached while still in the gas phase (gas-phase precipitation) as will be reviewed later. As can be expected, the mathematical modeling of these phenomena can be complicated.

The sequence of events taking place during a CVD reaction is shown graphically in Fig. 2.3 and can be summarized as follows:<sup>[1]</sup>

- Reactant gases enter the reactor by forced flow.
- Gases diffuse through the boundary layer.
- Gases come in contact with surface of substrate.
- Deposition reaction takes place on surface of substrate.
- Gaseous by-products of the reaction are diffused away from the surface, through the boundary layer.

These steps occur in the sequence shown and the slowest step determines the deposition rate. The rules of the boundary layer apply in most CVD depositions in the viscous flow range where pressure is relatively high. In cases where very low pressure is used (i.e., in the mTorr range), the rules are no longer applicable.

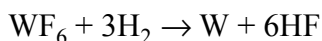


1. Diffusion in of reactants through boundary layer
2. Adsorption of reactants on substrate
3. Chemical reaction takes place
4. Desorption of adsorbed species
5. Diffusion out of by-products

**Figure 2.3.** Sequence of events during deposition.

### 3.2 Deposition in a CVD Flow Reactor

The sequence of events described above occurs at any given spot in a CVD flow reactor. As an example, one can consider the deposition of tungsten on the interior wall of a graphite tube by the hydrogen reduction of the fluoride as follows:



As shown schematically in Fig. 2.4a, the reactant gases are introduced in the upstream side, then flow down the reactor tube, and exhaust downstream through the vacuum pump.

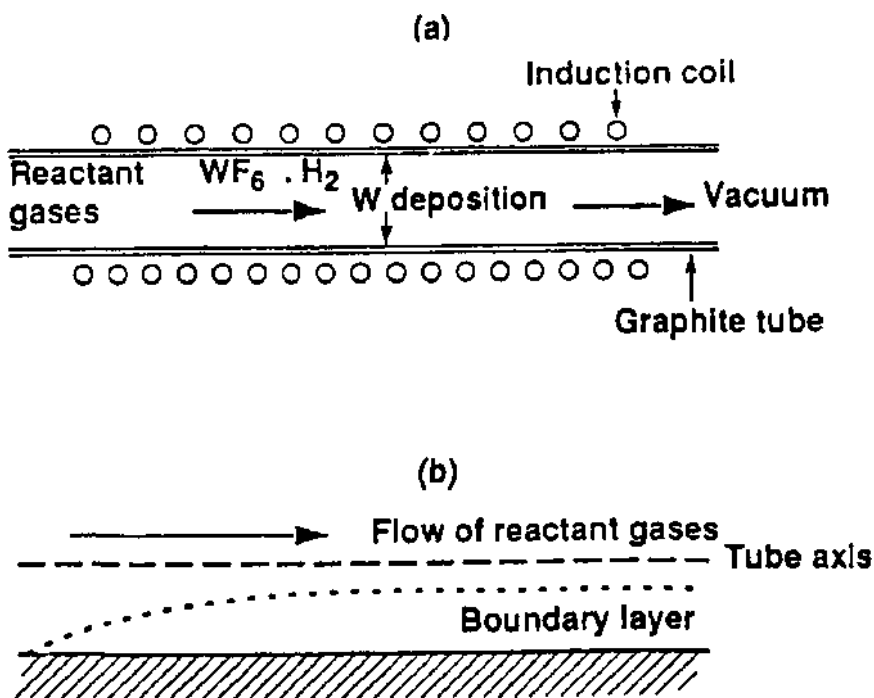


**Figure 2.4.** (a) Tungsten deposition in a tubular reactor, (b) boundary layer conditions.

### 3.3 Boundary Layer

The behavior of the gas as it flows down the tube is controlled by fluid mechanics and a complete investigation would be lengthy and outside the scope of this book. It is enough to say that the Reynolds number,  $R_e$ , which is a dimensionless parameter that characterizes the flow of a fluid, is such that the gas flow is generally laminar, although in some instances the laminar flow may be disturbed by convective-gas motion and may become turbulent.

In the case of laminar flow, the velocity of the gas at the deposition surface (the inner wall of the tube) is zero. The boundary is that region in which the flow velocity changes from zero at the wall to essentially that of the bulk gas away from the wall. This boundary layer starts at the inlet of the tube and increases in thickness until the flow becomes stabilized as shown in Fig. 2.4b. The reactant gases flowing above the boundary layer have to diffuse through this layer to reach the deposition surface as is shown in Fig. 2.3.

The thickness of the boundary layer,  $\Delta$ , is inversely proportional to the square root of the Reynolds number as follows:

$$\text{Eq. (4)} \quad \Delta = \sqrt{\frac{x}{R_e}}$$

$$\text{where: } R_e = \frac{\rho u_x}{\mu}$$

$\rho$  = mass density

$u$  = flow density

$x$  = distance from inlet in flow direction

$\mu$  = viscosity

This means that the thickness of the boundary layer increases with lower gas-flow velocity and with increased distance from the tube inlet.<sup>[14]</sup>

### 3.4 Gas Velocity

Under such conditions, it is possible to obtain an approximate visualization of the gas-flow pattern by using  $\text{TiO}_2$  smoke (generated when titanium chloride comes in contact with moist air), although thermal diffusion may keep the smoke particles away from the hot surface where a steep temperature gradient exists. Figure 2.5 shows a typical velocity pattern in a horizontal tube. As mentioned above, a steep velocity gradient is noticeable going from maximum velocity at the center of the tube to zero velocity at the surface of the wall. The gradient is also shallow at the entrance of the tube and increases gradually toward downstream.

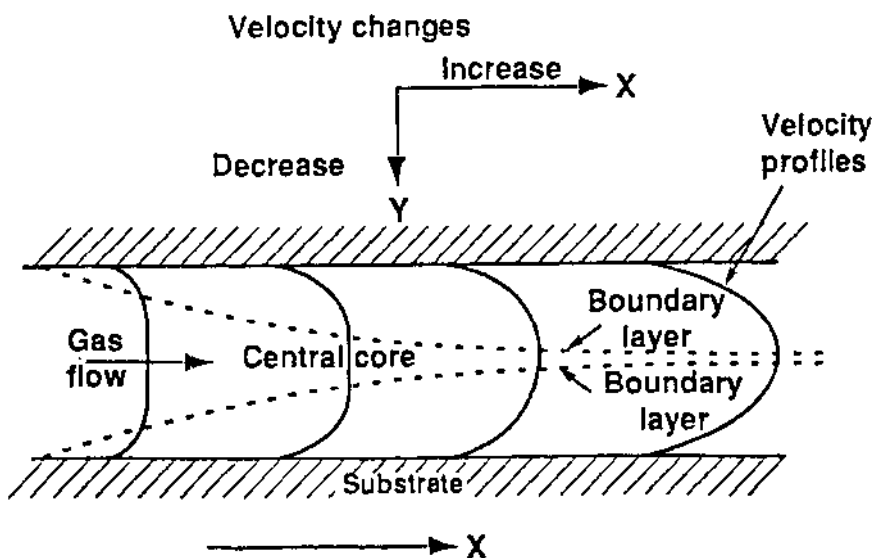


**Figure 2.5.** Boundary layer and velocity changes in a tube reactor, showing the graphs of velocity recorded at different positions on the tube.

### 3.5 Temperature

Figure 2.6 shows a typical temperature profile.<sup>[2]</sup> The temperature boundary layer is similar to the velocity layer. The flowing gases heat rapidly as they come in contact with the hot surface of the tube, resulting in a steep temperature gradient. The average temperature increases toward downstream.

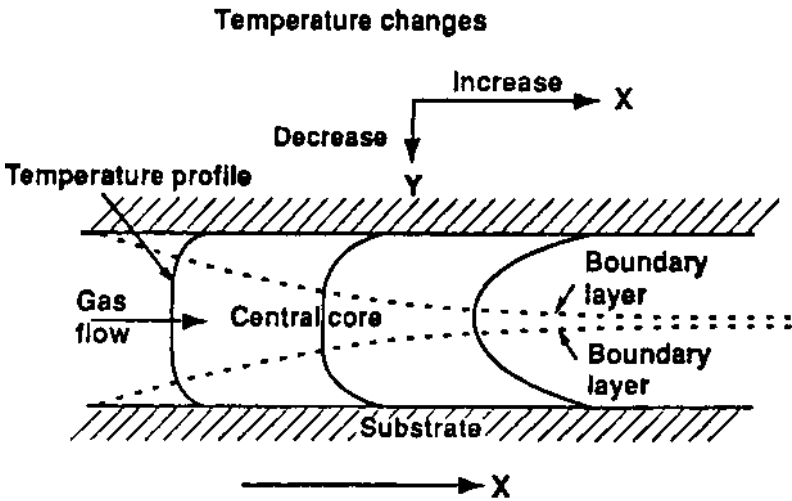


**Figure 2.6.** Temperature boundary layer and temperature changes in a tubular reactor, showing the graphs of temperature recorded at different positions on the tube.

### 3.6 Reactant-Gas Concentration

As the gases flow down the tube, they become gradually depleted as tungsten is deposited and the amount of the by-product gas, HF, increases in the boundary layer. This means that, at some point downstream, deposition will cease altogether when  $WF_6$  is no longer present. The reactant concentration is illustrated in Fig. 2.7.

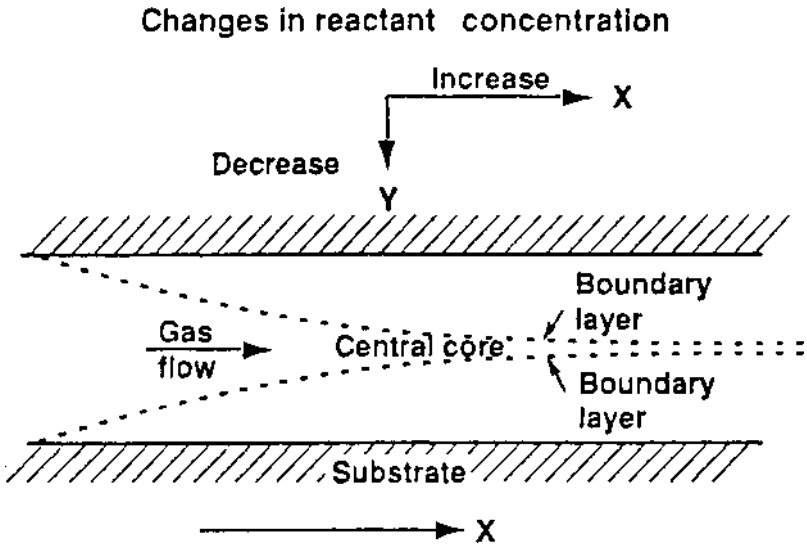


**Figure 2.7.** Changes in reactant concentration in a tubular reactor.

The boundary layers for these three variables (gas velocity, temperature, and concentration) may sometimes coincide, although in slow reactions, the profiles of velocity and temperature may be fully developed at an early stage while the deposition reaction is spread far downstream the tube.

As can be seen, conditions in a flowing reactor, even the simplest such as a tube, may be far from the thermodynamic equilibrium conditions predicted by the equilibrium computer programs. However, in the diffusion controlled range, it is possible to use as the driving force for diffusion, the difference between an assumed equi-

librium composition at the wall and the bulk-gas composition in the feed (adjusted for downstream depletion), to model some systems to a first approximation.

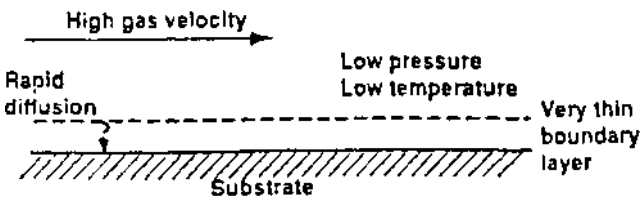
### 3.7 Rate-Limiting Steps

What is the rate limiting step of a CVD reaction? In other words, what factor controls the growth rate of the deposit? The answer to this question is critical since it will help to optimize the deposition reaction, obtain the fastest growth rate and, to some degree, control the nature of the deposit.

The rate-limiting step is generally determined by either the surface reaction kinetics or by mass transport.

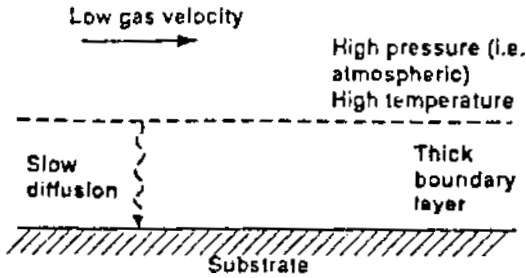
### 3.8 Surface-Reaction Kinetics

In the case of control by surface reaction kinetics, the rate is dependent on the amount of reactant gases available. As an example, one can visualize a CVD system where the temperature and the pressure are low. This means that the reaction occurs slowly because of the low temperature and there is a surplus of reactants at the surface since, because of the low pressure, the boundary layer is thin, the diffusion coefficients are large, and the reactants reach the deposition surface with ease as shown in Fig. 2.8a.



(a)

**Figure 2.8.** Rate-limiting steps in a CVD reaction (a) surface reaction kinetics control, (b) diffusion control.



(b)

**Figure 2.8.** (*Cont'd.*)

### 3.9 Mass Transport

When the process is limited by mass-transport phenomena, the controlling factors are the diffusion rate of the reactant through the boundary layer and the diffusion out through this layer of the gaseous by-products. This usually happens when pressure and temperature are high. As a result, the gas velocity is low as was shown above, and the boundary layer is thicker making it more difficult for the reactants to reach the deposition surface. Furthermore, the decomposition reaction occurs more rapidly since the temperature is higher and any molecule that reaches the surface reacts instantly. The diffusion rate through the boundary layer then becomes the rate limiting step as shown in Fig. 2.8b.

### 3.10 Control of Limiting Step

To summarize, the surface kinetics (or near surface kinetics) is the limiting step at lower temperature and diffusion is the rate limiting step at higher temperature. It is possible to switch from one rate-limiting step to the other by changing the temperature. This is illustrated in Fig. 2.9, where the Arrhenius plot (logarithm of the deposition rate vs. the reciprocal temperature) is shown for several reactions leading to the deposition of silicon,

using either  $\text{SiH}_4$ ,  $\text{SiH}_2\text{Cl}_2$ ,  $\text{SiHCl}_3$ , or  $\text{SiCl}_4$  as silicon sources in a hydrogen atmosphere.<sup>[15]</sup>

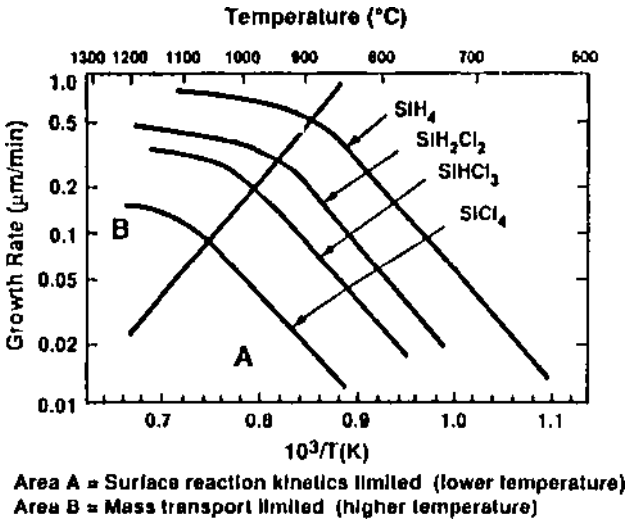


**Figure 2.9.** Arrhenius plot for silicon deposition using various precursors.

In the A sector (lower right), the deposition is controlled by surface-reaction kinetics as the rate-limiting step. In the B sector (upper left), the deposition is controlled by the mass-transport process and the growth rate is related linearly to the partial pressure of the silicon reactant in the carrier gas. Transition from one rate-control regime to the other is not sharp, but involves a transition zone where both are significant. The presence of a maximum in the curves in Area B would indicate the onset of gas-phase precipitation, where the substrate has become starved and the deposition rate decreased.

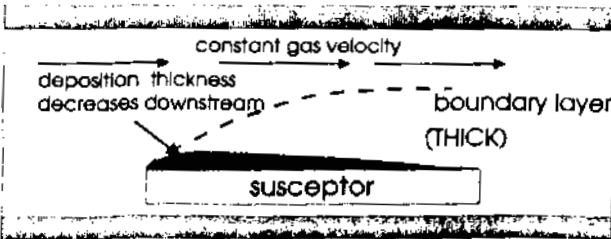
### 3.11 Pressure as Rate-Limiting Factor

Pressure is similar to temperature as a rate limiting factor since the diffusibility of a gas is inversely related to its pressure. For instance, lowering the pressure 760 Torr (1 atm) to 1 Torr increases the gas-phase transfer of reactants to the deposition surface and the

diffusion out of the by-products by more than 100 times. Clearly, at low pressure, the effect of mass-transfer variables is far less critical than at higher pressure.

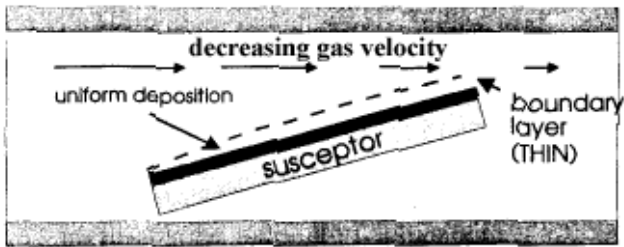
However, the gain may not be as large if the overall pressure decrease is at the expense of the partial pressure of reactant gas, since the kinetic rate (for first-order reactions) is proportional to the partial pressure of the reactant. Reducing the pressure by reducing the flow of carrier gas (or eliminating altogether) is a good alternative and is usually beneficial. At low pressure, surface reaction is the rate determining step and the mass-transfer variables are far less critical than at atmospheric pressure.

It can be now seen that, by proper manipulation of the process parameters and reactor geometry, it is possible to control the reaction and the deposition to a great degree. This is illustrated by the following example. In the deposition of tungsten in a tube mentioned in Sec. 3.2 above, the gas velocity is essentially constant and the boundary layer gradually increases in thickness toward downstream. This means that the thickness of the deposit will decrease as the distance from the tube inlet increases, as shown in Fig. 2.10a. This thickness decrease can be offset and a more constant thickness obtained simply by tilting the susceptor, as shown in Fig. 2.10b. This increases the gas velocity due the flow constriction; the Reynolds number goes up; the boundary layer decreases and the deposition rate is more uniform.<sup>[14]</sup>



(a)

**Figure 2.10.** Control of deposition uniformity in a tubular reactor (a) susceptor parallel to gas flow, (b) titled susceptor.



(b)

**Figure 2.10.** (Cont'd.)

### 3.12 Mathematical Expressions of the Kinetics of CVD

The flow-dynamics and mass-transport processes can be expressed mathematically and realistic models obtained to be used in the predictions of a CVD operation and in the design of reactors.<sup>[16]–[18]</sup> These models are designed to define the complex entrance effects and convection phenomena that occur in a reactor and solve the complete equations of heat, mass balance, and momentum. They can be used to optimize the design parameters of a CVD reactor such as susceptor geometry, tilt angle, flow rates, and others. To obtain a complete and thorough analysis, these models should be complemented with experimental observations, such as the flow patterns mentioned above and in situ diagnostic, such as laser Raman spectroscopy.<sup>[19]</sup>

## 4.0 GROWTH MECHANISM AND STRUCTURE OF DEPOSIT

In the previous sections, it was shown how thermodynamic and kinetic considerations govern a CVD reaction. In this section, the nature of the deposit, i.e., its microstructure and how it is controlled by the deposition conditions, is examined.

## 4.1 Deposition Mechanism and Epitaxy

The manner in which a film is formed on a surface by CVD is still a matter of controversy and several theories have been advanced to describe the phenomena.<sup>[2]</sup> A thermodynamic theory proposes that a solid nucleus is formed from supersaturated vapor as a result of the difference between the surface free energy and the bulk free energy of the nucleus. Another and newer theory is based on atomistic nucleation and combines chemical bonding of solid surfaces and statistical mechanics.<sup>[20]</sup> These theories are certainly valuable in themselves but considered outside the scope of this book.

There are, however, three important factors that control the nature and properties of the deposit to some degree which must be reviewed at this time: epitaxy, gas-phase precipitation, and thermal expansion.

## 4.2 Epitaxy

The nature of the deposit and the rate of nucleation at the very beginning of the deposition are affected, among other factors, by the nature of the substrate. A specific case is that of epitaxy where the structure of the substrate essentially controls the structure of the deposit.<sup>[2][15][20]</sup> Epitaxy can be defined as the growth of a crystalline film on a crystalline substrate, with the substrate acting as a seed crystal. When both substrate and deposit are of the same material (for instance silicon on silicon) or when their crystalline structures (lattice parameters) are identical or close, the phenomena is known as homoepitaxy. When the lattice parameters are different, it is heteroepitaxy. Epitaxial growth cannot occur if these structural differences are too great.

A schematic of epitaxial growth is shown in Fig. 2.11. As an example, it is possible to grow gallium arsenide epitaxially on silicon since the lattice parameters of the two materials are similar. On the other hand, deposition of indium phosphide on silicon is not possible since the lattice mismatch is 8%, which is too high. A solution is to use an intermediate buffer layer of gallium arsenide between the silicon and the indium phosphide. The lattice parameters of common semiconductor materials are shown in Fig. 2.12.

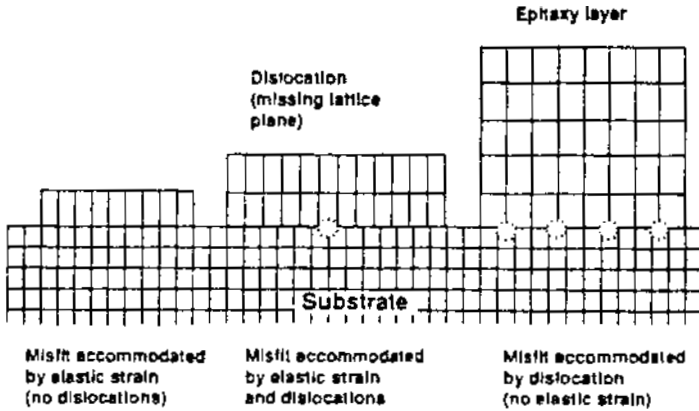


**Figure 2.11.** Epitaxy accommodations of lattice mismatch.

Generally, epitaxial films have superior properties and, whenever possible, epitaxial growth should be promoted. The epitaxial CVD of silicon and III–V and II–VI compounds is now a major process in the semiconductor industry and is expected to play an increasingly important part in improving the performance of semiconductor and optoelectronic designs (see Chs. 13–15).<sup>[22]</sup>

### 4.3 Gas Phase Precipitation

As mentioned previously, a CVD reaction may occur in the gas phase instead of at the substrate surface if the supersaturation of the reactive gases and the temperature are sufficiently high. This is generally detrimental because gas-phase precipitated particles, in the form of soot, become incorporated in the deposit, causing nonuniformity in the structure, surface roughness, and poor adhesion. In some cases, gas-phase precipitation is used purposely, such as in the production of extremely fine powders (see Ch. 19).

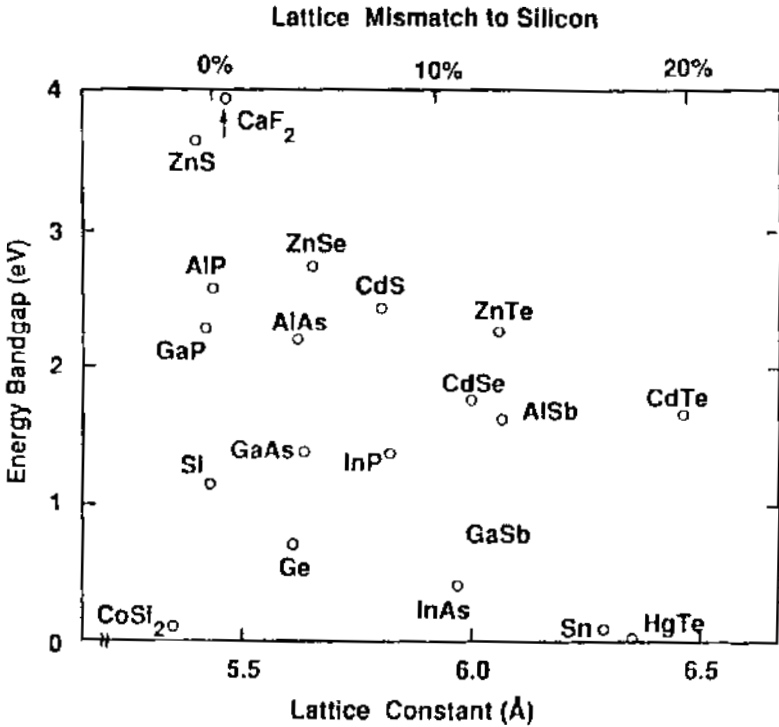


Figure 2.12. Bandgap and lattice constant of semiconductor materials.

#### 4.4 Thermal Expansion

Large stresses can be generated in a CVD coating during the cooling period from deposition temperature to room temperature, if there is a substantial difference between the coefficient of thermal expansion (CTE) of the deposit and that of the substrate. These stresses may cause cracking and spalling of the coating. If differences are large, it may be necessary to use a buffer coating with an intermediate CTE or with high ductility. Deposition processes which

do not require high temperatures, such as MOCVD or plasma CVD, should also be considered (see Ch. 4 and 5). Table 2.1 lists the CTE of typical CVD materials and substrates.

#### 4.5 Structure and Morphology of CVD Materials

The properties of a CVD material are directly related to the nature of its structure which is in turn controlled by the deposition conditions. In this section and the next, the relationship between properties, structure, and deposition conditions is examined.

The structure of a CVD material can be classified into three major types which are shown schematically in Fig. 2.13.<sup>[23]</sup> In Zone (A), the structure consists of columnar grains which are capped by a domelike top. In Zone (B), the structure is also columnar but more faceted and angular. In Zone (C), it consists of fine accost grains. Examples of these structures are shown in Fig. 2.14.<sup>[24]</sup> This is the CVD equivalent of the structural model for vacuum-evaporated films first introduced by Movchan and Demshishin.<sup>[25]</sup>

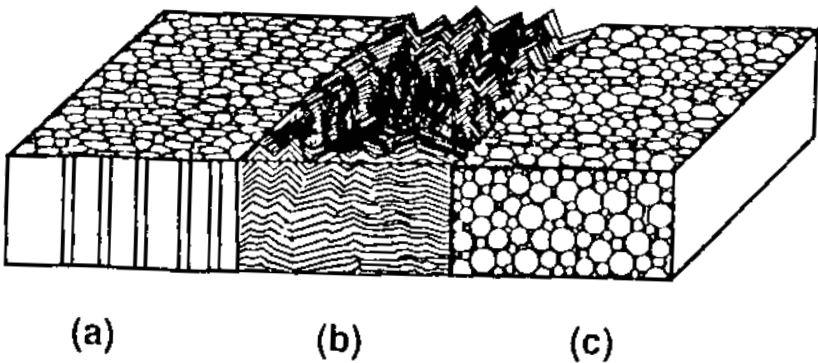
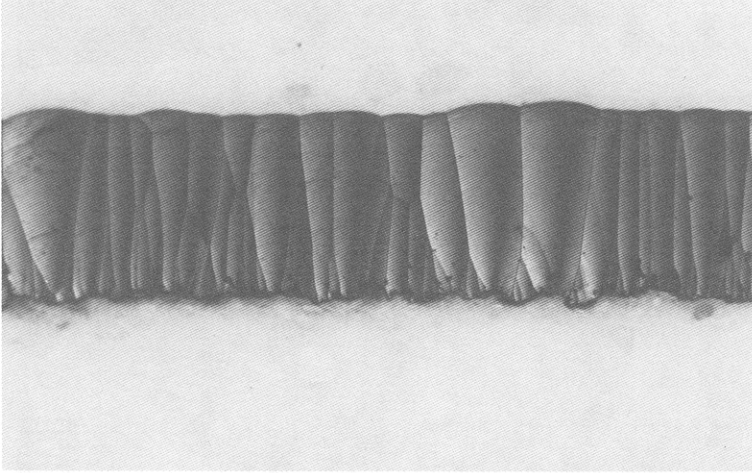


**Figure 2.13.** Schematic of structures obtained by CVD: (a) columnar grains with domed tops, (b) faceted columnar grains, (c) equiaxed fine grains.

**Table 2.1**  
**Coefficient of Thermal Expansion (CTE) of Typical CVD Materials**  
**and Substrates**

Materials	CTE (ppm/°C) 25–300°C
<b>Metals</b>	
Aluminum	23.5
Gold	14.2
Iridium	6
Molybdenum	5
Niobium	7
Steel (carbon)	12
Stainless Steel (302)	17.3
Tantalum	6.5
Titanium	9
Tungsten	4.5
<b>Non Metallic Elements</b>	
Carbon, hot-pressed	5.4
Carbon-carbon	0.5
Silicon	3.8
<b>Ceramics</b>	
Alumina	8.3
Boron carbide	4.5
Boron nitride	7.5
Chromia	8
Hafnia	7
Magnesia	13
Molybdenum disilicide	8.25
Silicon carbide	3.9
Silicon nitride	2.45
Silicon oxide	0.5
Titanium carbide	7.6
Titanium diboride	6.6
Titanium nitride	9.5
Tungsten carbide	4.5
Tungsten disilicide	6.6

Note: Reported values of CTE's often vary widely. The values listed here are an average from several sources.

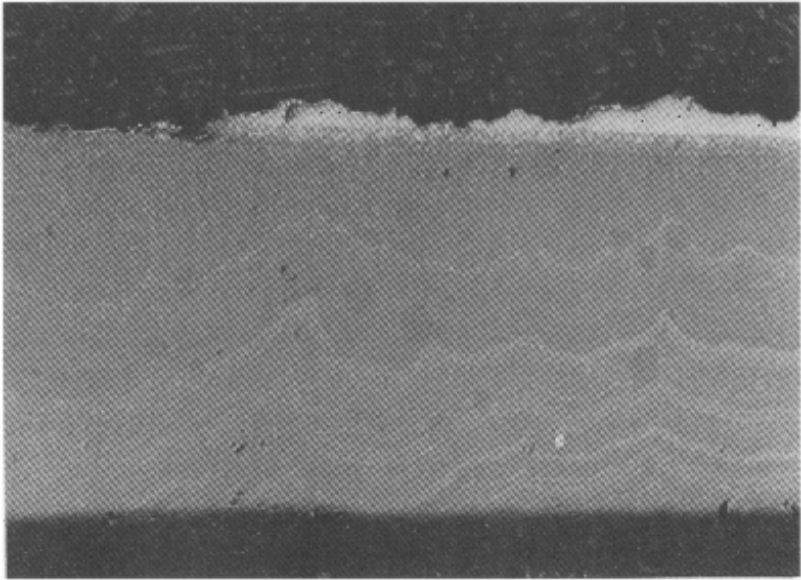


(a)

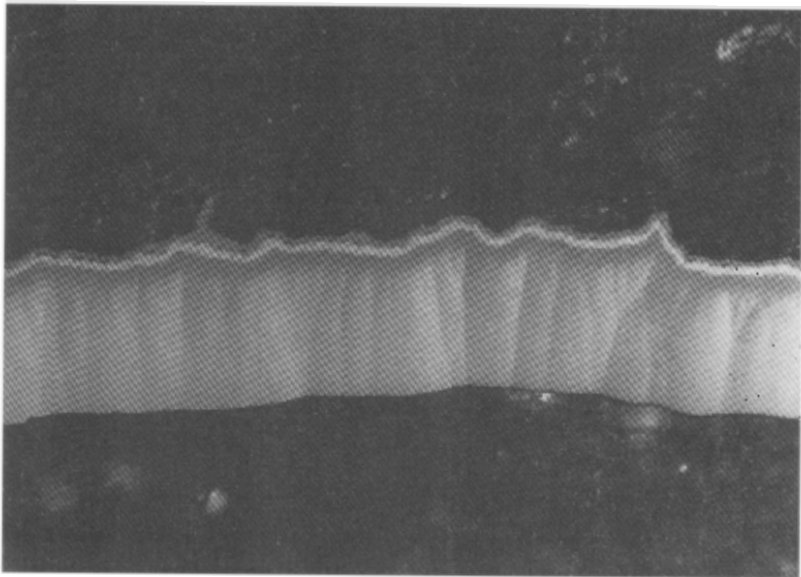


(b)

**Figure 2.14.** Examples of CVD structures: (a) columnar grains with domed tops, (b) faceted columnar grains, (c) equiaxed fine grains, (d) mixed structures. (Source: Ultramet, Pacoima, CA.)



(c)



(d)

**Figure 2.14.** (*Cont'd.*)

As might be expected, the microstructure varies depending on the material being deposited. In general, ceramics obtained by CVD such as  $\text{SiO}_2$ ,  $\text{Al}_2\text{O}_3$ ,  $\text{Si}_3\text{N}_4$ , and most dielectric materials tend to be amorphous or, at least, have a very small grain microstructure (Type C). Metal deposits tend to be more crystalline with the typical columnar structure of type (A) or (B). The crystal size of the deposits is also a function of deposition conditions, especially temperature. Generally, the most desirable structure for load-bearing use is the fine accost (C), which usually has the highest mechanical properties, such as hardness and fracture toughness.

More often than not, a deposited structure will include two and sometimes all three types. This usually happens in thick deposits where a uniform structure is more difficult to obtain.

#### **4.6 Control of CVD Microstructure**

It is possible to control the nature of a CVD structure by the proper manipulation of the deposition parameters such as temperature, pressure, supersaturation, and the selection of the CVD reaction.

Pressure controls the thickness of the boundary layer and consequently the degree of diffusion as was shown above. By operating at low pressure, the diffusion process can be minimized and surface kinetics becomes rate controlling. Under these conditions, deposited structures tend to be fine-grained, which is usually a desirable condition (Fig. 2.13c). Fine-grained structures can also be obtained at low temperature and high supersaturation as well as low pressure.

At higher temperatures, deposits tend to be columnar (Fig. 2.13 a and b) as a result of uninterrupted grain growth toward the reactant source. The structure is also often dependent on the thickness of the deposit. For instance, grain size will increase as the thickness increases. A columnar-grain structure develops, which becomes more pronounced as the film becomes thicker.

Columnar structures are usually undesirable as the deleterious effects of grain growth and columnar formation can be considerable. They may lead to structural, chemical, and electrical anisotropy and the rapid diffusion of impurities along the grain boundaries. It is possible to reduce or eliminate columnar deposits and obtain fine-grain accost growth by mechanical means such as rubbing or brushing at regular intervals to renucleate the deposition surface. This approach has been demonstrated in the deposition of tungsten.<sup>[13]</sup> However, it is not generally practical, particularly when substrates of complex geometry are used.

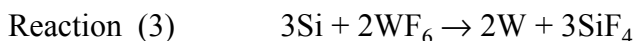
Another approach is the control of grain growth by chemical means.<sup>[26][27]</sup> In the deposition of tungsten for instance, a fine-grain equiaxial growth is obtained by depositing alternating layers of tungsten and silicon. Typically a layer of tungsten, approximately 100 nm thick, is deposited using the hydrogen reduction of  $WF_6$  at 550°C and a pressure of a few Torr as follows:



A 15 nm thick layer of silicon is then deposited by the thermal decomposition of silane at the same temperature and pressure as follows:



$WF_6$  is then reintroduced in the system and the thin layer of silicon is reduced as follows:



After the silicon is completely reduced, Reaction (3) stops and Reaction (1) is resumed. The temporary deposition of sacrificial silicon interrupts the tungsten grain growth as new nucleation sites are created. Larger grain and columnar growth are essentially eliminated

and a fine-grain structure is the result. A similar process can be used for the deposition of rhenium and other metals.

## REFERENCES

1. Spear, K. E., "Thermochemical Modeling of Steady-State CVD Process," *Proc. 9th. Int. Conf. on CVD*, (M. Robinson, et al., eds.), pp. 81–97, Electrochem. Soc., Pennington, NJ 08534 (1984)
2. Kern, W., and Ban, W. S., "Chemical Vapor Deposition of Inorganic Thin Films," *Thin Film Processes*, (J. L. Vossen and W. Kern, eds.), pp. 257–331, Academic Press, New York (1987)
3. Gokoglu, S. A., "Chemical Vapor Deposition Modeling—An Assessment of Current Status," *Proc. 11th. Int. Conf. on CVD*, (K. Spears and G. Cullen, eds.), pp. 1–9, Electrochem. Soc., Pennington, NJ 08534 (1990)
4. Pierson, H. O., "The CVD of  $TiB_2$  from Diborane," *Thin Solid Films*, 72:511–516 (1980)
5. Chase, M. W., *JANAF Thermochemical Tables*, 13(1), American Chem. Soc. & Am. Inst. of Physics (1985)
6. Many sources of thermodynamic data are now available including the following:
  - Wagman, D. D., "The NBS Tables of Chemical Thermodynamic Properties," *J. Phys. Chem. Ref. Data* 11 and supplements (1982)
  - Barin, I., and Knacke, O., *Thermochemical Properties of Inorganic Substances*, Springer, Berlin (1983)
  - Hultgren, R., *Selected Values of the Thermodynamic Properties of the Elements*, Am. Soc. for Metals, Metals Park, OH (1973)

- Mills, K. C., *Thermodynamic Data for Inorganic Sulphides, Selenides and Tellurides*, Butterworth, London (1974)
- 7. Carlsson, J. O., "Chemical Vapor Deposition," *Handbook of Deposition Technologies for Films and Coatings*, (R. Bunshah, ed.), Noyes Publications, Westwood, NJ (1994)
- 8. Nolang, B., "Equilibrium Computations and Their Application to CVD Systems," *Proc. of 5th. European Conf. on CVD*, (J. O. Carlsson and J. Lindstrom, eds.), pp. 107–115, University of Uppsala, Sweden (1985)
- 9. Gordon, S., and McBride, B. J., NASA Publication SP273 (1971)
- 10. Eriksson, G., *Acta Chem. Scandia*, 25:2651–2658 (1971)
- 11. Besmann, T. M., "SOLGASMIX-PV, A Computer Program to Calculate Equilibrium Relationship in Complex Chemical Systems," ORNL/TM-5775, *Oak Ridge National Laboratory*, Oak Ridge, TN (1977)
- 12. EKVICALC and EKVIBASE, *Svensk Energi Data*, Agersta, S-740 22 Balinge, Sweden
- 13. Blocher, J. M., Jr., "Chemical Vapor Deposition," *Deposition Technologies for Films and Coatings*, (R. Bunshah, ed.), pp. 348–351, Noyes Publications, Park Ridge, NJ (1982)
- 14. Sherman, A., *Chemical Vapor Deposition for Electronics*, Noyes Publications, Park Ridge, NJ (1987)
- 15. Pearce, C. W., "Epitaxy," *VLSI Technology*, (S. M. Sze, ed.), McGraw-Hill Book Co., New York (1983)
- 16. Jensen, K. F., "Modelling of Chemical Vapor Deposition Reactors," *Proc. 9th. Int. Conf. on CVD*, (M. Robinson, et al., eds.), pp. 3–20, Electrochem. Soc., Pennington, NJ 08534 (1984)
- 17. Rosenberger, F., "Flow Dynamics and Modelling of CVD," *Proc. 10th. Int. Conf. on CVD*, (G. W. Cullen, ed.), pp. 193–203, Electrochem. Soc., Pennington, NJ, 08534 (1987)

18. He, Y., and Sahai, Y., "Three-Dimensional Mathematical Modeling of Transport Processes in CVD Reactors," *Proc. 10th. Int. Conf. on CVD*, (G. W. Cullen, ed.), Electrochem. Soc., Pennington, NJ (1987)
19. Breiland, W. G., Ho, P., and Coltrin, M. E., "Laser Diagnostics of Silicon CVD: In Situ Measurements and Comparisons with Model Predictions," *Proc. 10th. Int. Conf. on CVD*, (G. W. Cullen, ed.), pp. 912–924, Electrochem. Soc., Pennington, NJ 08534 (1987)
20. Gretz, R. D., and Hirth, J. P., "Nucleation and Growth Process in CVD," *CVD of Refractory Metals Alloys and Compounds*, pp. 73–97, Am. Nuclear Soc., Hinsdale, Ill. (1967)
21. Venables, J. A., and Price, G. L., *Epitaxial Growth*, (J. W. Matthews, ed.), Pt. B, p. 382, Academic Press, New York (1975)
22. Wu, C., et al., "Epitaxial Growth of 3c-SiC on Si(111) from HMDS," *J. Crystal Growth*, 158(4):480–490 (Feb. 1996)
23. Stinton, D. P., Bessman, T. M., and Lowden, R., "Advanced Ceramics by Chemical Vapor Deposition Techniques," *Cer. Bul.*, 67(2):350–355 (1988)
24. Photographs by permission of Ultramet, Pacoima, CA 91331
25. Movchan, B. A., and Demchishin, A. V., *Fisika Metall.*, 28:653 (1959)
26. Green, M., et al., "The Formation and Structure of CVD W Films Produced by the Si Reduction of  $WF_6$ ," *J. Electrochem. Soc.*, 134(9):2285–92 (1987)
27. Kamins T. I., et al., *J. Electrochem. Soc.*, 133(12):2555–9 (1986)